



Article

UV/Advanced Oxidation Process for Removing Humic Acid from Natural Water: Comparison of Different Methods and Effect of External Factors

Qingchao Shen ^{1,2}, Xiaosan Song ^{1,2,*} , Jishuo Fan ^{1,2} , Cheng Chen ^{1,2} and Zhuohao Li ^{1,2}

¹ School of Environmental and Municipal Engineering, Lanzhou Jiaotong University, No. 88 Anning West Road, Lanzhou 730070, China; 13964762817@163.com (Q.S.); van1131@163.com (J.F.); 17513188534@163.com (C.C.); 17339901314@163.com (Z.L.)

² Key Laboratory of Yellow River Water Environment in Gansu Province, Lanzhou Jiaotong University, No. 88 Anning West Road, Lanzhou 730070, China

* Correspondence: songxs@mail.lzjtu.cn

Abstract: Humic acid (HA) is an organic compound naturally present in aquatic environments. It has been found to have detrimental effects on water color, the transport of heavy metals, and the elimination of disinfection by-products (DBPs), thereby exerting an impact on human health. This study introduced four synergistic ultraviolet/advanced oxidation processes (UV/AOPs) systems aimed at eliminating HA from water. The research explored the effect of solution pH, duration of illumination, initial reactant concentration, and oxidant concentration on the degradation of HA. The results indicated that the mineralization rate achieved by individual UV or oxidant systems was less than 15%, which is significantly lower compared to UV/AOPs systems. Among these methods, the UV/peroxymonosulfate (UV/PMS) process demonstrated the highest effectiveness, achieving a mineralization rate of 94.15%. UV/peroxydisulfate (UV/PDS) and UV/sodium percarbonate (SPC) were subsequently implemented, with UV/sulfite (S(IV)) demonstrating the lowest effectiveness at 19.8%. Optimal degradation efficiency was achieved when the initial concentration of HA was 10 mg/L, the concentration of PMS was 3 mmol/L, and the initial pH was set at 5, with an illumination time of 180 min. This experimental setup resulted in high degradation efficiencies for chemical oxygen demand (COD), UV₂₅₄, and HA, reaching 96.32%, 97.34%, and 92.09%, respectively. The energy efficiency of this process (*EE/O*) was measured at 0.0149 (kWh)/m³, indicating the capability of the UV/PMS system to efficiently degrade and mineralize HA in water. This offers theoretical guidance for the engineered implementation of a UV/PAM process in the treatment of HA.

Keywords: humic acid; ultraviolet/advanced oxidation processes; techniques; influencing factors



Citation: Shen, Q.; Song, X.; Fan, J.; Chen, C.; Li, Z. UV/Advanced Oxidation Process for Removing Humic Acid from Natural Water: Comparison of Different Methods and Effect of External Factors. *Water* **2024**, *16*, 1815. <https://doi.org/10.3390/w16131815>

Academic Editors: Antonio Zuerro, Zacharias Frontistis, José A. Peres, Juan García Rodríguez, Gassan Hodaifa, Joaquín R. Dominguez and Mha Albqmi

Received: 4 June 2024

Revised: 20 June 2024

Accepted: 22 June 2024

Published: 26 June 2024



Copyright: © 2024 by the authors. Licensee MDPI, Basel, Switzerland. This article is an open access article distributed under the terms and conditions of the Creative Commons Attribution (CC BY) license (<https://creativecommons.org/licenses/by/4.0/>).

1. Introduction

In China, water resources are significantly contaminated, primarily by organic pollutants, with natural organic matter (NOM) serving as a major pollution source. NOM constitutes a crucial element of aquatic ecosystems and is commonly present in natural water sources, with levels typically varying between 0.1 mg/L and 20 mg/L, demonstrating a progressive escalation [1,2]. Elevated concentrations of NOM impose significant challenges on nearby water treatment plants and ecosystems. In an aqueous environment, the constituents of NOM, specifically humic acid (HA), exhibit a significant ability to chelate heavy metals, leading to the formation of organic–metal complexes. This affects the transportation, bioavailability, and toxicity of heavy metals [3,4]. Although the presence of HA in drinking water does not pose a direct threat to human health, it is responsible for water discoloration and the emission of a strong, unpleasant odor. Common disinfectants utilized in water treatment facilities, such as chlorine or chloramines, undergo a reaction with HA to produce halogenated compounds (trihalomethanes (THMs), haloacetic acids

(HAAs), and halogenated furanones (HFs) [5]), consequently elevating the potential risk of cancer [6].

In recent years, elevated concentrations of aromatic halogenated disinfection by-products (DBPs) have been identified in chlorinated drinking water. These compounds have shown developmental toxicity and growth inhibitory effects that are more pronounced compared to aliphatic halogenated DBPs [7]. Epidemiological studies in humans and toxicological research in animals have established correlations between the consumption of chlorinated drinking water and adverse effects on cancer, reproduction, and development. United States Environmental Protection Agency (EPA) currently establishes the maximum contaminant levels for total THMs and HAAs at 80 ppb and 60 ppb, respectively. In contrast, the United Kingdom adheres to a THM standard of 100 ppb [8]. During the process of water treatment, the interaction of organic substances with metal ions and minerals leads to an increase in the solubility of heavy metals. This phenomenon also necessitates higher chemical dosages, which in turn diminishes treatment effectiveness and results in the production of larger quantities of sludge and DBPs [9]. Furthermore, the existence of humic substances in the water treatment facilities has implications on the efficacy of treatment processes (e.g., coagulation-settling efficiency, coagulant and oxidant dosages, and operational equipment), and fosters the growth of bacteria and the development of biofilms in the water distribution network, thereby giving rise to public health concerns regarding sanitation. Consequently, the management of HA in untreated water has garnered significant interest from the potable water sector [10,11].

The main strategies for eliminating HA encompass a variety of approaches. These include physical methods such as adsorption [12] and filtration [13], chemical techniques such as coagulation [14], electrolysis [15], and oxidation [16,17], as well as biological processes [18]. The advantages and disadvantages of these methods are outlined in Table 1. Advanced oxidation processes (AOPs) have attracted considerable interest in recent years because of their operational simplicity, high efficiency, lack of secondary pollution, and efficacy in decreasing THM formation [19]. AOPs operate through the production of highly oxidative radicals, such as hydroxyl ($\bullet\text{OH}$) and sulfate ($\text{SO}_4^{\bullet-}$) [20], which facilitate the oxidation and decomposition of organic pollutants present in water. However, relying only on AOPs for the degradation of HA frequently proves ineffective in attaining optimal results. Therefore, they are commonly integrated with other technologies, such as ultraviolet/AOPs (UV/AOPs). This integrated method not only efficiently eliminates HA but also minimizes the generation of DBPs, thereby exerting a beneficial effect on the management of organic fouling in water treatment procedures [21].

Table 1. Advantages and disadvantages of different methods for NOM degradation.

Method	Advantages	Disadvantages
Adsorption	① High NOM degradation efficiency ② Simple design and easy operation	① Frequent replacement and regeneration of adsorbents increase costs ② Saturated adsorbents require disposal, causing secondary pollution
Coagulation	Strong adaptability with high NOM degradation efficiency	Causes secondary pollution
Biological	① Can remove biodegradable components of NOM ② Relatively environmentally friendly, no extra chemicals	① Requires additional nutrients ② Poor environmental adaptability
Electrochemical	① No secondary pollution, environmentally friendly ② No need for additional chemicals	High energy consumption
Membrane Filtration	① Simple process, easy to automate, reliable operation ② Low energy consumption	① Severe membrane fouling ② High membrane cost
Advanced Oxidation	① Efficient degradation of organic matter ② Applicable to various water bodies, widely adaptable	① Complex operation, requires monitoring and control of reaction conditions ② Residual oxidants may be toxic

UV-activated AOPs are currently utilized for the elimination of organic compounds from water. However, there is a limited availability of studies assessing their efficacy, particularly for removing HA. Furthermore, there is a scarcity of research on determining the

most effective oxidant for the treatment of HA using UV/AOPs. This study examines the efficacy of four oxidants—peroxymonosulfate (PMS), peroxydisulfate (PDS), sodium percarbonate (SPC), and sulfite (S(IV))—when activated by UV light to identify the most efficient AOP for removing HA. This research aims to investigate the effect of initial concentration of HA, oxidant concentration, initial pH, and reaction time on the decontamination of HA. The results of this study are expected to offer insights for the practical implementation of UV/AOP technologies in the treatment of HA.

2. Methods

2.1. Reagents and Equipment

2.1.1. Reagents

HA (fulvic acid, FA $\geq 90\%$) was obtained from Shanghai Macklin Biochemical Co., Ltd. (Shanghai, China); Sodium persulfate ($\text{Na}_2\text{S}_2\text{O}_8$) and anhydrous sodium S(IV) were procured from Shanghai Macklin Biochemical Co., Ltd.; potassium PMS and SPC were acquired from Shanghai Titan Technology Co., Ltd. (Shanghai, China); sulfuric acid (H_2SO_4) and hydrochloric acid (HCl) were obtained from Shanghai National Medicines Reagents Co., Ltd. (Shanghai, China); sodium hydroxide (NaOH) was provided by Sigma-Aldrich Co., Ltd. (Shanghai, China). All chemicals utilized in the study were of analytical grade and did not necessitate additional purification.

2.1.2. Experimental Equipment

To facilitate the development of experiments in this study, a specialized experimental apparatus utilizing UV oxidation was created (Shandong University of Architecture, Jinan, China). The schematic and actual representations of this device are depicted in Figures 1 and 2, respectively. The device is primarily composed of an upper sealing flange, dual-layer acrylic glass tubes, and an innermost glass sleeve. The flange is the location where an inlet for water addition (reagent addition) is situated. The gap between the inner and outer glass tubes functions as a condensation cycling water system, where the water inlet and outlet are strategically positioned at the bottom and top of the outer tube, respectively. The inner glass tube is designed to be removable and includes a drainage outlet at the bottom as well as two sampling ports located at the mid-upper section. This equipment has the capacity to treat a maximum of 4 L of water in a single session.

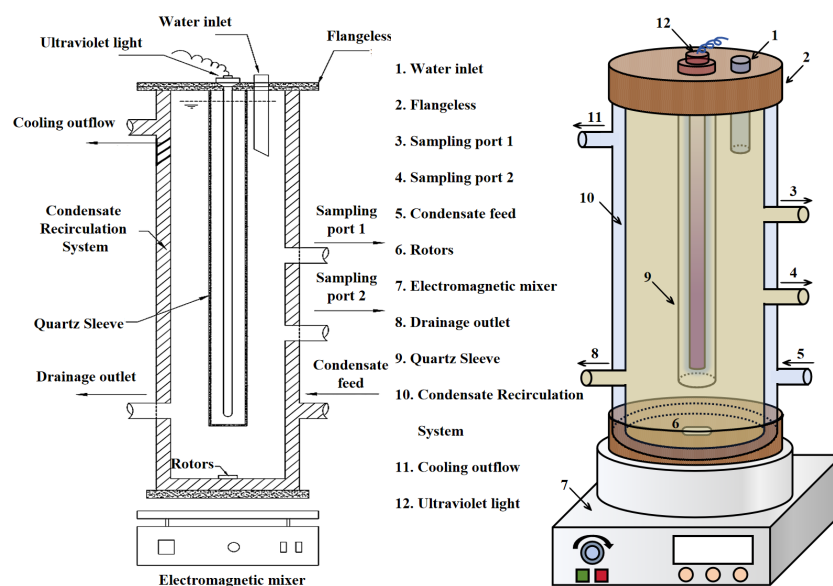


Figure 1. Structure of the advanced oxidation reaction device.

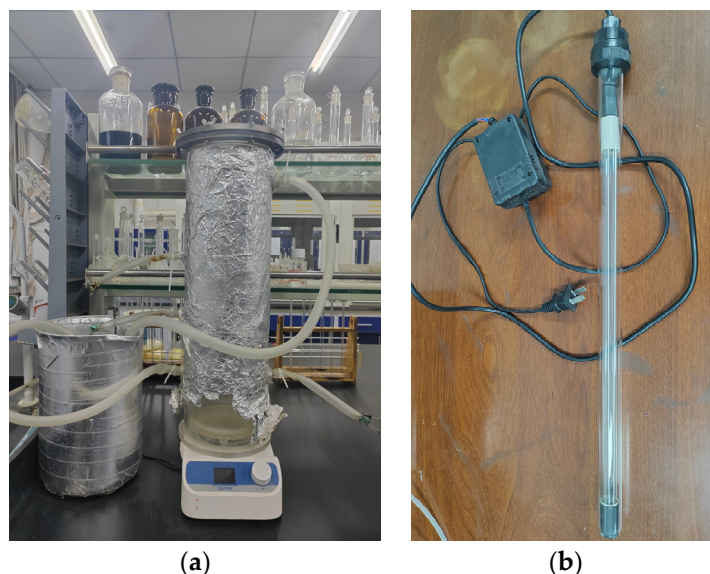


Figure 2. Diagram of the experimental setup: (a) advanced oxidation reaction setup; (b) UV lamp.

The design of this experimental apparatus is simple and intuitive for users. The glass tube of the UV lamp can be removed, facilitating the simple substitution with lamps of different specifications and types. Sampling ports are strategically positioned at various heights on the device to facilitate convenient sampling. A supplementary port is situated at the upper part of the device to facilitate the convenient introduction of reagents. The external glass layer is equipped with a condensing water circulation system that helps reduce temperature elevation caused by radiation when the UV lamp is in operation. The full submersible UV lamp used in the test was OSRAM, model HNS 4P SE, with a power of 20 W, a rated operating voltage of 220 V, and an average UV radiation intensity of 3.28 mW/cm^2 as measured by a radiometer. The outer diameter of the UV lamp casing was 25 mm, the diameter at the head was 18 mm, the diameter of the glass tube was 15.5 mm, and the wavelength was 254 nm.

2.2. Experimental Indicators and Testing Methods

2.2.1. Routine Indicator Measurement

(1) Physical Indicators

Temperature variations and pH levels in the water samples were observed through the utilization of a thermometer and a pH meter, respectively. During the experiments, the pH range was controlled by utilizing 0.05 mol/L NaOH and 0.05 mol/L H_2SO_4 buffer solutions. Prior to conducting the experiments, the pH meter underwent calibration using standard solutions with pH values of 4.0, 6.86, and 9.18.

(2) Chemical Oxygen Demand (COD)

COD was quantified utilizing the acidic potassium permanganate method, following the guidelines outlined in the standard GB 11892-89 [22]. This approach is applicable for water samples with chloride ion concentrations not exceeding 30 mg/L. When the permanganate index surpasses 10 mg/L, it is advisable to collect smaller volumes of the water sample and dilute it before conducting the test.

2.2.2. Dissolved Organic Carbon (DOC) Measurement

DOC was quantified utilizing a total organic carbon (TOC) analyzer (MULTI N/C 2100, Analytik Jena, Germany, purchased in Beijing, China). Water samples underwent filtration using a $0.45 \mu\text{m}$ filter membrane prior to analysis to quantify the concentration of dissolved organic carbon. This section of the analysis employed a differential subtraction method to reduce errors associated with the measurement of organic carbon.

2.2.3. UV₂₅₄ Measurement

Temperature variations and pH levels in the water samples were observed through the utilization of a thermometer and a pH meter, respectively. During the experiments, the pH range was controlled by utilizing 0.05 mol/L NaOH and 0.05 mol/L H₂SO₄ buffer solutions. Prior to conducting the experiments, the pH meter underwent calibration using standard solutions with pH values of 4.0, 6.86, and 9.18.

2.2.4. Other Relevant Indicators

(1) Organic Matter Degradation Rate

$$\eta = \frac{C_0 - C_t}{C_0} \times 100\% \quad (1)$$

where η represents the degradation rate of organic matter (%); C_0 represents the initial concentration of organic matter (mg/L); and C_t represents the concentration of organic matter at time t (mg/L).

(2) Specific Electrical Energy per Order (EE/O)

$$EE/O = \frac{P \times T}{60 \times V \times \log(C_0/C) \times 1000} \quad (2)$$

where EE/O represents the specific electrical energy per order ((kWh)/m³); P represents the power of illumination (W); t represents the reaction time (min); V represents the volume of treated water (m³); and C_0 and C represent the initial and final concentrations of HA (mg/L), respectively.

2.3. Experimental Operation and Procedures

Before initiating the experiment, it is necessary to allow a 20-minute preheating period for the UV lamp. Before initiating the device, it is placed on a magnetic stirrer to guarantee homogeneous mixing and uphold a consistent temperature throughout the reaction. The preheated UV lamp is subsequently inserted into the internal sleeve, and the circulating water system is then attached at the inlet. The reaction solution and associated chemicals are introduced into the glass tube to guarantee uniform exposure of the water sample to UV radiation. The apparatus is enveloped in opaque aluminum foil to reduce external light interference and shield the experimenter's eyes from potential harm caused by UV radiation. Once the UV lamp is activated, in conjunction with the condensation circulation system and the magnetic stirrer, the chemical reaction can commence. The reaction temperature is consistently maintained at 25 ± 3 °C throughout the duration of the experiment. Each experimental group carries out 3 parallel tests. An oxidant with a specific concentration is introduced into the reactor, followed by the activation of the magnetic stirrer at a consistent speed of 630 rpm. Tap water is utilized for condensation purposes to maintain a stable reaction temperature. After the completion of the reaction under different conditions, a specific volume of the reaction solution is gathered, and the reaction is halted for subsequent analysis and measurement. In order to ensure the authenticity and reliability of the data, all the data in this experiment were obtained by taking the mean value from three parallel experiments, and the error bars were added in the plotting process to indicate the range of error.

3. Results and Discussion

3.1. Degradation Efficiency of HA by UV/PMS in Aqueous Solutions

Under the experimental conditions of UV radiation intensity at 3.28 mW/cm², initial solution pH at 7, initial concentration of HA at 10 mg/L, and the addition of 3 mmol/L PMS, the solution temperature was controlled at 25 ± 3 °C with a stirring rate of 630 rpm. The reaction was carried out for a duration of 180 min. The degradation effects of HA were

examined using three experimental configurations: isolated UV irradiation, isolated PMS treatment, and the combined UV/PMS process.

Figure 3 illustrates the degradation rates when subjected to isolated conditions of UV irradiation and PMS oxidation. For the isolated UV treatment, the degradation rates for COD, TOC, and UV_{254} were 11.01%, 9.84%, and 23.33%, respectively. For the oxidation of isolated PMS, the degradation rates for COD, TOC, and UV_{254} were 10.8%, 19.91%, and 27.7%, respectively. In the isolated UV system, the introduction of UV energy facilitated the cleavage of specific chemical bonds in the pollutants [23], leading to the partial degradation of organic compounds even in the absence of an oxidizing agent. UV photolysis of H_2O , however, produces a minimal quantity of $\bullet OH$ radicals with restricted oxidative potential, leading to decreased degradation rates for HA. In the isolated PMS system, the stability of PMS is relatively high, and its lower redox potential ($E^0 = 1.82$ V) limits the oxidation and degradation of organic compounds, resulting in incomplete removal of organics [24]. Consequently, both isolated UV and isolated PMS processes demonstrated low degradation efficiencies for COD, TOC, and UV_{254} , indicating their suboptimal performance in removing HA.

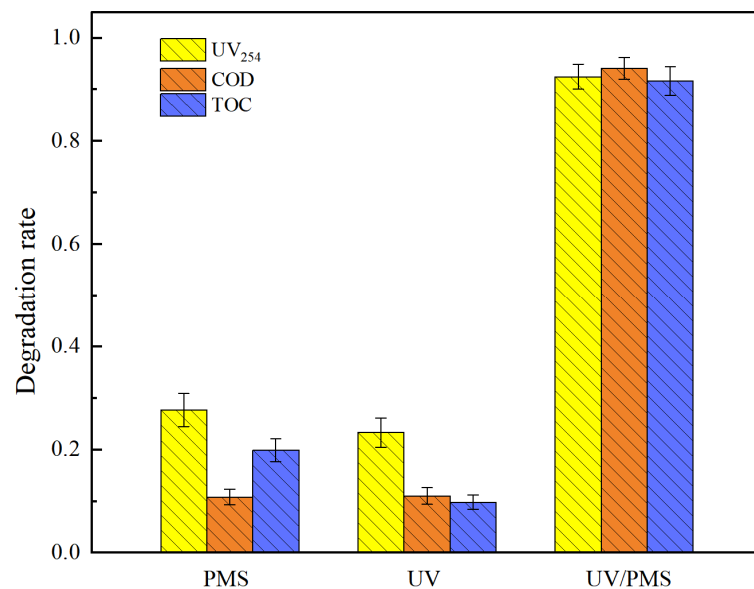


Figure 3. Degradation of HA by isolated UV, isolated PMS, and UV/PMS.

Under the same experimental conditions, the UV/PMS process exhibited significantly higher degradation rates for COD, TOC, and UV_{254} compared to the individual UV or PMS processes, achieving rates of 94.12%, 91.65%, and 92.51%, respectively. In Figure 4, the energy input from UV radiation causes O-O bond in PMS to split. This activation process involves external energy exceeding the bond energy (140~213.3 kJ/mol) [25], leading to the cleavage of the peroxide bond in PMS and the generation of $SO_4^{\bullet -}$ radicals and $\bullet OH$. These radicals are potent oxidizing agents that can rapidly degrade various pollutants [26–28]. Therefore, the UV/PMS process is more advantageous for HA degradation compared to the use of UV or PMS alone. Additionally, the UV/PMS process can oxidize organic compounds that are not effectively degraded by PMS alone.

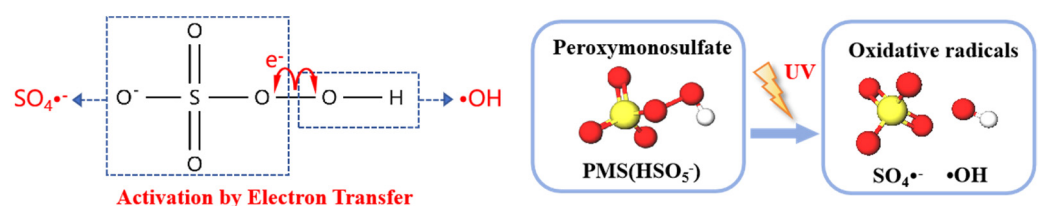


Figure 4. Activation of PMS through electron and energy transfer processes [29].

3.2. Degradation Efficiency of HA by UV/PDS in Aqueous Solutions

Under experimental conditions, a UV radiation intensity of 3.28 mW/cm^2 , a solution temperature of $25 \pm 3 \text{ }^\circ\text{C}$, an initial solution pH of 7, and an initial concentration of 10 mg/L of HA, 3 mmol/L of PDS was introduced. The reaction lasted for 180 min with a stirring rate of 630 rpm. The degradation effects of HA were examined using 3 experimental configurations: isolated UV, isolated PDS, and a combined UV/PDS process. The study aimed to evaluate the effectiveness of UV/PDS AOP in degrading HA.

In Figure 5, when subjected to isolated UV irradiation, the degradation rates for COD, TOC, and UV_{254} were 11.01%, 9.84%, and 23.33% respectively. Conversely, under isolated PDS oxidation, the degradation rates were 24.14% for COD, 16.28% for TOC, and 13.27% for UV_{254} . However, when subjected to identical experimental conditions, the UV/PDS process increased the degradation rates to 89.81% for UV_{254} , 93.60% for COD, and 89.53% for TOC. In comparison to the individual processes of UV and PDS, the combined UV/PDS process significantly enhanced the mineralization rate of HA. In the UV/PDS system, the PDS compound is activated under UV radiation, leading to the generation of $\text{SO}_4^{\cdot-}$ radicals possessing a high oxidative potential (Figure 6). These radicals participate in electron transfer, addition, and hydrogen abstraction reactions with organic pollutants. This process breaks down the organic matter into smaller, more degradable molecules, leading to increased degradation rates of organic compounds [30].

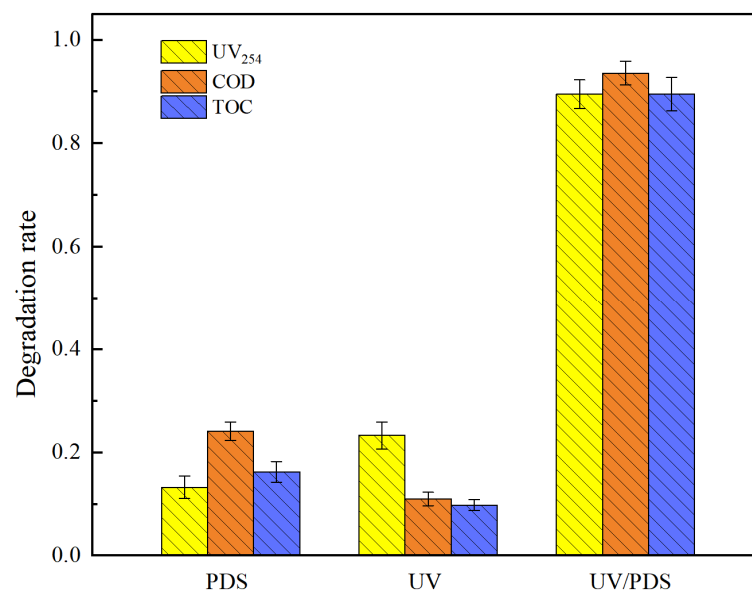


Figure 5. Degradation of HA by isolated UV, isolated PDS, and UV/PDS.

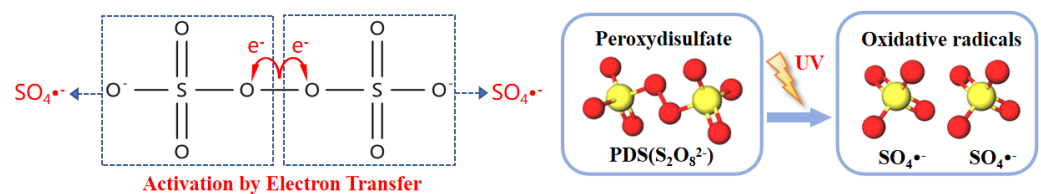


Figure 6. Activation of PDS through electron and energy transfer processes [29].

3.3. Degradation Efficiency of HA by UV/SPC in Aqueous Solutions

The experiment was carried out under conditions with a UV radiation intensity of 3.28 mW/cm^2 , an initial solution pH of 7, and an initial concentration of HA at 10 mg/L . SPC was introduced into the solution at a concentration of 3 mmol/L . The solution temperature was controlled at $25 \pm 3 \text{ }^\circ\text{C}$, while the stirring speed was adjusted to 630 rpm. The duration of the reaction was 180 min. Figure 7 depicts the degradation efficiencies of HA

through three processes: isolated UV treatment, isolated SPC treatment, and the combined UV/SPC process.

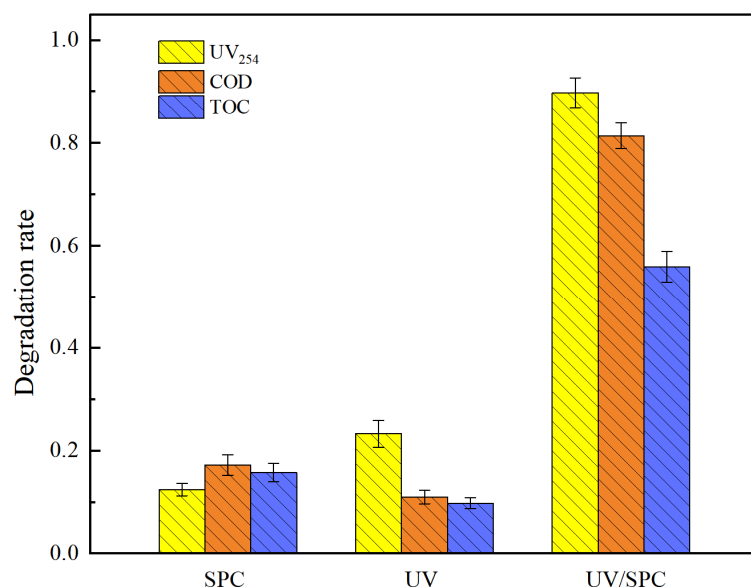
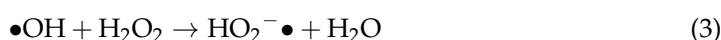


Figure 7. Degradation of organic matter by isolated UV, isolated SPC, and UV/SPC.

In Figure 7, during isolated SPC oxidation, the degradation rates for COD, TOC, and UV₂₅₄ were 17.21%, 15.79%, and 12.48% respectively. Conversely, under isolated UV irradiation, the degradation rates were 11.01% for COD, 9.84% for TOC, and 23.33% for UV₂₅₄. However, when subjected to identical experimental conditions, the integrated UV/SPC process demonstrated degradation efficiencies of 89.81% for UV₂₅₄, 81.47% for COD, and 56.00% for TOC. This suggests that the UV/SPC process offers superior degradation efficiencies for organic compounds in comparison to the separate processes of SPC and UV. However, its efficacy is not as pronounced as that of the UV/PMS and UV/PDS systems. The relatively low rate of TOC degradation indicates the breakdown of large molecular organic compounds into smaller molecules, suggesting that HA was not fully mineralized. The decomposition of organic compounds takes place as SPC dissolves in water, leading to the production of hydrogen peroxide (H₂O₂). Upon exposure to UV radiation, H₂O₂ becomes activated and generates highly reactive •OH radicals.

Yuan et al. [31] illustrated in their research on the elimination of HA from water through UV/SPC that H₂O₂ generated from the breakdown of SPC is probably the main supplier of oxidative capability in UV/SPC system. Additionally, the gradual degradation of SPC in water results in the continuous production of H₂O₂, thereby inhibiting the self-decomposition of H₂O₂ and augmenting the oxidative efficiency of UV/SPC system. With an increase in the concentration of SPC, there is a corresponding increase in the generation of highly reactive species such as •OH radicals, thereby enhancing the degradation of HA. However, an overabundance of SPC could potentially scavenge •OH, leading to the formation of hydroperoxy radicals (HO₂[•]) (Equation (3)) [32,33]. Considering that HO₂[•] exhibits lower oxidative potency, an excess of SPC may reduce the effectiveness of the system in eliminating HA.



3.4. Degradation Efficiency of HA by UV/S(IV) in Aqueous Solutions

The experiment was carried out under specific conditions, including a UV radiation intensity of 3.28 mW/cm², an initial solution pH of 7, and an initial concentration of HA at 10 mg/L. S(IV) was introduced into the solution at a concentration of 3 mmol/L, while the solution temperature was controlled at 25 ± 3 °C, and the stirring speed was adjusted

to 630 rpm. The reaction persisted for a duration of 180 min. The efficiency of organic matter decomposition was examined using three experimental configurations: isolated UV irradiation, isolated S(IV) treatment, and a combined UV/S(IV) process. Sampling and analytical results demonstrating the degradation effects of HA by these three processes are depicted in Figure 8.

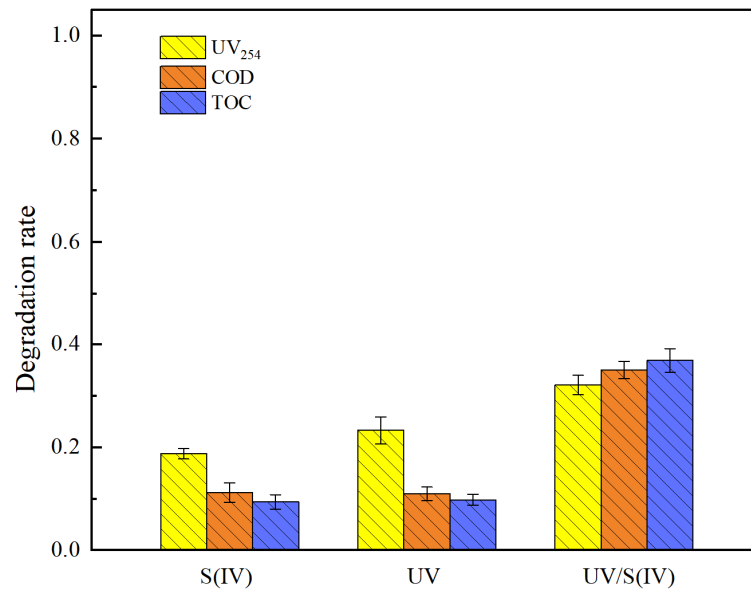
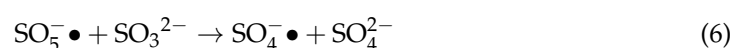


Figure 8. Degradation of organic matter by isolated UV, isolated S(IV), and UV/S(IV).

In Figure 8, during isolated S(IV) oxidation, the degradation rates for COD, UV₂₅₄, and TOC were 11.22%, 18.76%, and 9.44%, respectively. Conversely, under isolated UV irradiation, the degradation rates were 11.01% for COD, 23.33% for UV₂₅₄, and 9.84% for TOC. Under identical experimental conditions, the UV/S(IV) process resulted in degradation rates of 32.14% for UV₂₅₄, 35.06% for COD, and 36.88% for TOC. A comparative analysis indicates that UV/S(IV) process does not substantially improve the degradation efficiencies in comparison to the individual treatments, suggesting suboptimal efficiency in organic degradation. The results indicate that there is minimal degradation of HA within UV/S(IV) system. This is attributed to the low generation of radicals and the intricate, high molecular weight structure of HA, which encompasses numerous functional groups that pose challenges for decomposition. In UV/S(IV) system, the main reactive species are S(IV) radicals ($\text{SO}_3^- \bullet$) and hydrated electrons (e^-_{aq}) as denoted in Equation (4). In the presence of oxygen, $\text{SO}_3^- \bullet$ species can undergo further transformation into PMS ($\text{SO}_5^- \bullet$). The e^-_{aq} is rapidly captured as a result of its high reaction rate constant ($\geq 10^{10} \text{ M}^{-1} \cdot \text{s}^{-1}$) [34], leading to the formation of superoxide radicals ($\text{O}_2^- \bullet$). The oxidative potential of $\text{O}_2^- \bullet$ is lower than that of $\bullet\text{OH}$ and $\text{SO}_4^- \bullet$. Consequently, the UV/S(IV) collaborative system exhibits a significantly reduced capacity for organic degradation in comparison to the other collaborative systems previously examined. Furthermore, as demonstrated in Equations (5) to (7), in aerobic environments, the UV/S(IV) system has the potential to produce $\text{SO}_4^- \bullet$. Therefore, the reactive species $\text{SO}_3^- \bullet/\text{SO}_5^- \bullet$, $\text{O}_2^- \bullet$, and $\text{SO}_4^- \bullet$ have the potential to enhance the degradation of HA [35].



3.5. Comparison of Oxidant Efficacy in HA Degradation

A comparative study was conducted under identical experimental conditions to assess the degradation effectiveness of PMS, PDS, sodium SPC, and S(IV) in oxidative synergy systems for HA. The degradation effects of each synergistic system were examined, and the results are illustrated in Figure 9. In UV/oxidant processes, the degradation of HA by varying concentrations of oxidants exhibited pseudo-first-order kinetics. The specific first-order kinetic constants (k_{obs}) are shown in Table 2.

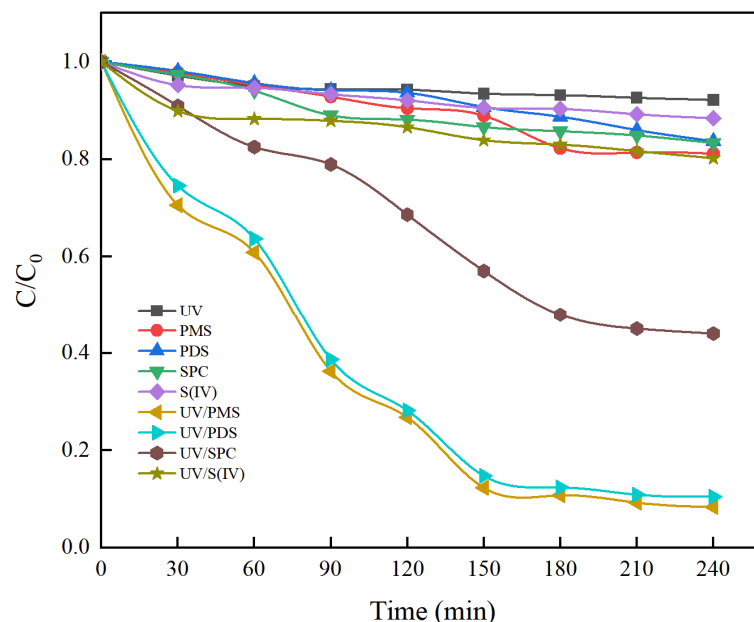


Figure 9. Mineralization effects of different processes on HA.

Table 2. Comparison of rate constants and economic efficiency for different processes.

System	First-Order Kinetic Equation	k_{obs} (min^{-1})	R^2	EE/O ($(\text{kWh})/\text{m}^{-3}$)
UV/PMS	$\text{Ln}(C_0/C) = 0.01034t + 0.1516$	0.01034	0.928	0.0157
UV/PDS	$\text{Ln}(C_0/C) = 0.0094t + 0.1355$	0.00940	0.919	0.0204
UV/SPC	$\text{Ln}(C_0/C) = 0.00342t + 0.0147$	0.00342	0.975	0.0561
UV/S(IV)	$\text{Ln}(C_0/C) = 0.00051t + 0.0077$	0.00051	0.978	0.3750

Under experimental conditions, a UV radiation intensity of $3.28 \text{ mW}/\text{cm}^2$, an initial solution pH of 7, an initial HA concentration of $10 \text{ mg}/\text{L}$, and the addition of $3 \text{ mmol}/\text{L}$ AOPs were employed. The reaction was carried out at a solution temperature of $25 \pm 3 \text{ }^\circ\text{C}$ with a stirring speed of 630 rpm for 240 min. In Figure 9, the individual processes (e.g., UV, PMS, PDS, SPC, and S(IV)) employed for HA degradation resulted in minimal mineralization. C/C_0 values for HA were 92.16%, 81.17%, 83.72%, 83.33%, and 88.43% for UV, PMS, PDS, SPC, and S(IV) processes, respectively. Consequently, the mineralization rates were below 15%. In contrast, UV/AOPs synergistic systems such as UV/PMS, UV/PDS, and UV/SPC exhibited enhanced mineralization efficiency, as evidenced by C/C_0 values of 5.85%, 10.47%, and 44.00%, resulting in mineralization rates of 94.15%, 89.53%, and 56%, respectively. Among the synergistic processes, UV/S(IV) exhibited the lowest performance, achieving a C/C_0 value of 80.20% and a mineralization rate of merely 19.8%. A comparative analysis reveals that depending exclusively on UV irradiation or oxidants is inadequate for producing a significant quantity of radicals essential for the efficient mineralization of HA. The activation of oxidants via external energy input is crucial for the generation of highly oxidative radicals. These radicals play a key role in breaking down large organic molecules into inorganic substances. This underscores the synergistic effect of integrating UV/AOPs, which enhances the breakdown of organic substances.

In Figure 10, following a 240-minute reaction period in the oxidation systems, UV_{254} degradation efficiencies for the UV/PMS, UV/PDS, UV/SPC, and UV/S(IV) processes were 95.07%, 89.81%, 87.64%, and 32.14%, respectively. The degradation efficiencies of COD were 96.26%, 93.16%, 81.47%, and 35.06%, respectively. The comparison indicates that the highest UV_{254} and COD degradation efficiencies were observed in the UV/PMS and UV/PDS processes, while the UV/S(IV) process exhibited the lowest efficiency, followed by the UV/SPC process. Analysis of the first-order kinetic equations fitted in Table 1 reveals that k_{obs} for UV/PMS treatment was determined to be 0.01034 min^{-1} , signifying the highest degradation efficiency. The rate constant for the UV/PDS system was determined to be 0.00940 min^{-1} , which was marginally lower compared to the rate constant of the UV/PMS system. The k_{obs} values for the UV/SPC and UV/S(IV) synergistic processes were 0.00342 min^{-1} and 0.00051 min^{-1} , respectively. These values suggest lower rates of organic matter degradation in comparison to the UV/PMS and UV/PDS processes.

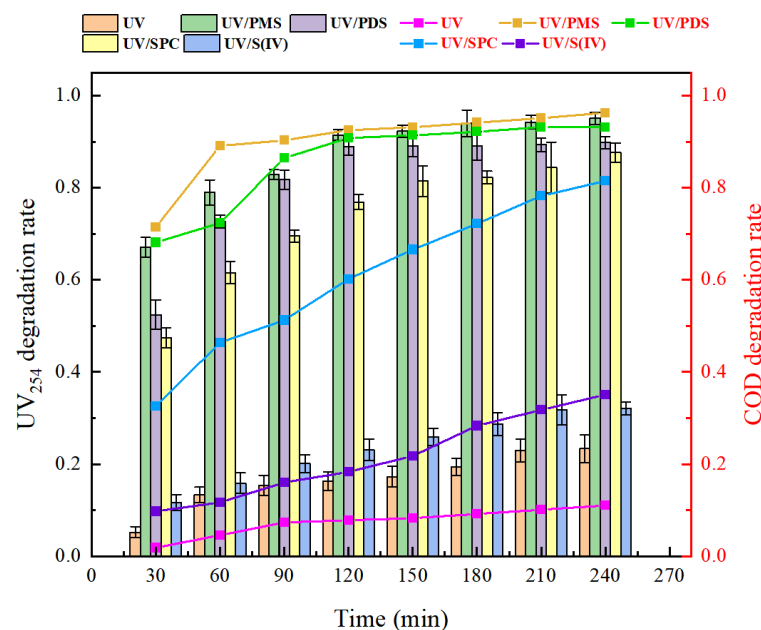


Figure 10. Degradation effects of organic matter by different synergistic processes.

The comparative analysis indicated that UV/PMS process demonstrated superior mineralization and degradation efficiency for HA. PMS exhibits superior oxidizing properties due to its dipole-asymmetric structure and high oxidation potential. Its low molecular orbital energy enhances its electron acceptance capabilities [36], thereby promoting easier activation and the generation of crucial reactive radicals. These radicals efficiently eliminate organic substances from water. While PDS also demonstrates favorable oxidative characteristics, its symmetrical molecular configuration enhances its stability and makes it more challenging to trigger the release of $SO_4^{\cdot-}$. Consequently, a higher amount of UV radiation energy is necessary to produce radicals, as evidenced in Table 1. This elucidates the reason behind the higher EE/O for PDS (0.0204 (kWh)/m^3) compared to PMS (0.0157 (kWh)/m^3). Subsequent to PMS and PDS, SPC and S(IV) demonstrate elevated EE/O values of 0.0561 (kWh)/m^3 and 0.3750 (kWh)/m^3 , respectively.

Upon evaluation of the degradation efficiency of organic matter, mineralization rates, and the economic analysis of specific electrical energy consumption, it can be concluded that the UV/PMS synergistic system represents the optimal option for the elimination of HA. Subsequent to UV/PMS, the UV/PDS synergistic system and UV/SPC synergistic system have demonstrated effectiveness, while the UV/S(IV) synergistic system has shown to be the least effective.

3.6. Effect of External Conditions on the UV/PMS Process for HA Degradation

This study examines the effect of the initial solution pH, duration of illumination, concentration of oxidant, and concentration of HA on the efficiency of the UV/PMS process for removing HA. The particular effect mechanisms were examined to ascertain the most favorable operational parameters.

3.6.1. Effect of Initial Solution pH on HA Degradation

The initial pH value of the solution affects the molecular form, solubility of HA, radical generation, and activation of PMS [37,38]. This experiment investigated the degradation of HA under various initial pH conditions (3, 5, 7, 9, 11). Under the specified experimental parameters, including a UV radiation intensity of 3.28 mW/cm^2 , an initial concentration of 10 mg/L of HA, the addition of 3 mmol/L of PMS, a solution temperature held at $25 \pm 3 \text{ }^\circ\text{C}$, and a stirring speed of 630 rpm , the reaction was carried out for 180 min while varying the initial pH values. The results of the sampling and detection are depicted in Figure 11.

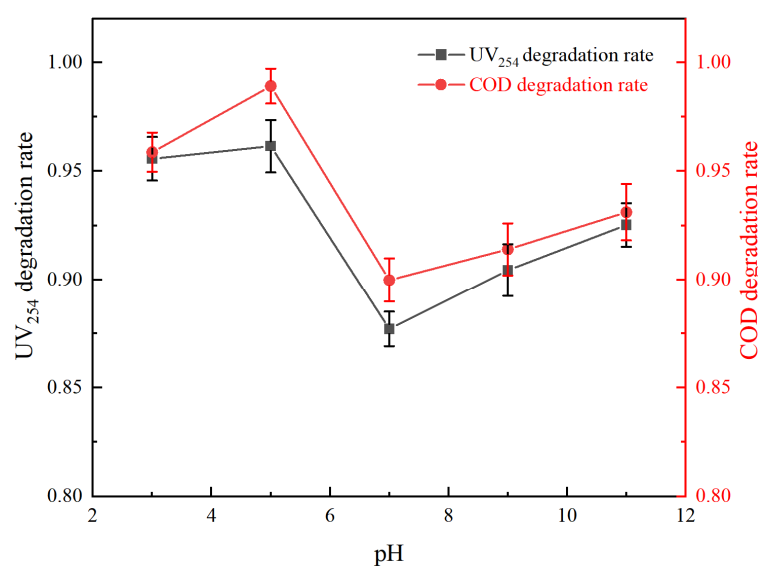
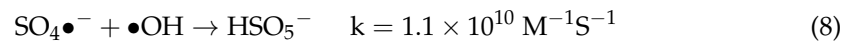


Figure 11. Effect of initial solution pH on degradation of HA in UV/PMS.

In Figure 11, the pH level exerts an impact on the elimination of HA. At a pH of 5, the degradation efficiency of organic matter was maximized, with UV₂₅₄ and COD degradation efficiencies reaching 96.15% and 98.92%, respectively. This resulted in nearly complete mineralization of HA in the solution. The subsequent most significant achievement was observed at a pH of 3, with UV₂₅₄ and COD degradation efficiencies reaching 95.58% and 95.88%, respectively. For pH values within the range of 7 to 11, the rates of UV₂₅₄ and COD degradation were marginally lower compared to those observed in acidic solutions. However, with an increase in pH, the degradation efficiencies exhibited a gradual upward trajectory, peaking at 92.53% and 93.12% at pH 11. The correlation coefficients (R^2) presented in Table 3 demonstrate that the degradation efficiency of HA under various pH conditions adheres to pseudo-first-order reaction kinetics. The first-order kinetic constants indicate that the rate of organic matter degradation was highest at pH = 5, followed by pH = 3, pH = 11, pH = 9, and pH = 7. The calculated results align with the data depicted in Figure 11.

Under conditions of high acidity, molecules of HA remain neutral, thereby augmenting their photochemical activity in comparison to conditions that are neutral or alkaline [39]. An initial acidic pH level enhances light absorption and photochemical reactions, consequently facilitating the efficient decomposition of HA when exposed to UV irradiation. During the alkaline activation of PMS, the main reactive species produced include $\bullet\text{OH}$ radicals, singlet oxygen ($^1\text{O}_2$), and $\text{O}_2^- \bullet$, which exhibit lower oxidative potentials in comparison to $\text{SO}_4^- \bullet$. Furthermore, in alkaline environments, the reaction between $\text{SO}_4^- \bullet$ and

•OH diminishes the oxidation potential of UV-activated persulfates (Equation (8)) [40,41]. This leads to a decrease in the oxidative capacity of UV/PMS at elevated pH values (7~11) in contrast to lower pH values (3~5) [42]. Consequently, slightly acidic conditions are more conducive to the degradation of HA in UV/PMS reaction system, resulting in the highest degradation efficiency for organic matter.



There was a decrease in pH levels towards the conclusion of this study. This phenomenon may be ascribed to the conversion of OH^- to •OH throughout the reaction and the potential generation of acidic compounds within the system, resulting in a decline in pH.

Table 3. Kinetic fitting of HA degradation at different pH levels.

HA	First-Order Kinetic Equation	k_{obs} (min^{-1})	R^2
3	$\text{Ln}(C_0/C) = 0.01467t + 0.0414$	0.01467	0.9868
5	$\text{Ln}(C_0/C) = 0.01763t + 0.0585$	0.01763	0.9850
7	$\text{Ln}(C_0/C) = 0.00912t + 0.0573$	0.00912	0.9856
9	$\text{Ln}(C_0/C) = 0.01249t + 0.0483$	0.01249	0.9907
11	$\text{Ln}(C_0/C) = 0.0139t + 0.05940$	0.01390	0.9808

3.6.2. Effect of Illumination Time on HA Degradation

Under the specified experimental parameters, including a UV radiation intensity of $3.28 \text{ mW}/\text{cm}^2$, an initial concentration of $10 \text{ mg}/\text{L}$ of HA, the presence of $3 \text{ mmol}/\text{L}$ of PMS, a solution temperature held at $25 \pm 3 \text{ }^\circ\text{C}$, and a stirring speed of 630 rpm , the reaction proceeded for 180 min at the pre-established optimal initial pH. This study aimed to investigate the effect of varying illumination durations on the degradation of HA through the UV/PMS process. The results are illustrated in Figure 12.

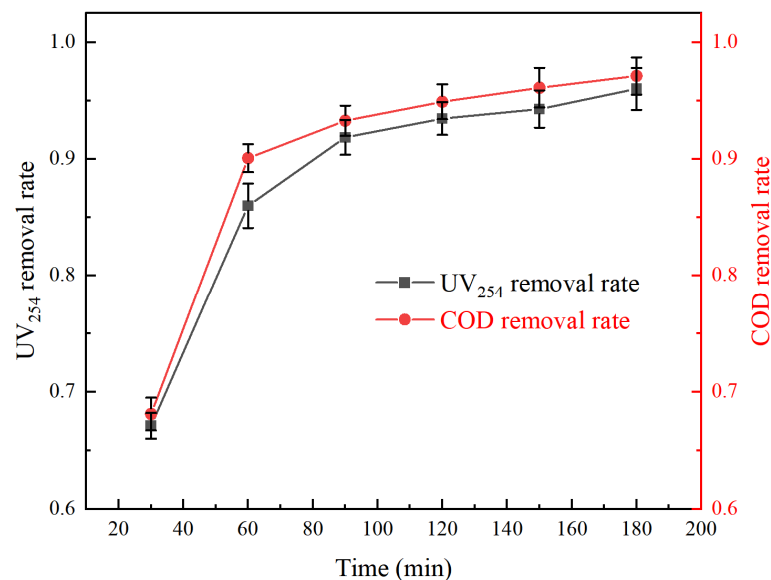


Figure 12. Effect of illumination time on degradation efficiency of organic matter.

In Figure 12, the degradation efficiencies of UV₂₅₄ and COD exhibited a gradual increase with extended illumination time. After 90 min, there was a deceleration in the rate of increase, suggesting a positive correlation between the degradation efficiency of HA in the UV/PMS synergistic process and the duration of illumination. At the conclusion of the experiment, the elimination percentages for UV₂₅₄ and COD stood at 96.02% and 97.12%,

respectively, while the presence of HA in the solution led to near-complete mineralization. Figure 13 demonstrates that an extended exposure to light resulted in a transition of the solution's color from dark brown to light yellow. After a duration of 90 min, it was significant that the solution exhibited a nearly transparent appearance. This indicates that prolonged exposure to light results in the generation of additional reactive radicals, thereby augmenting the mineralization rate of HA [43].

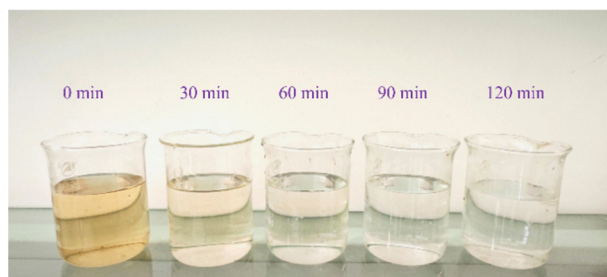


Figure 13. Actual images of HA degradation process solutions from 0 min to 120 min.

3.6.3. Effect of Oxidant Concentration on HA Degradation

The concentration of the oxidant (i.e., PMS) exerts an impact on the degradation efficacy of HA. Higher concentrations of oxidants can lead to an increased generation of oxidative radicals, consequently augmenting the degradation process. This study seeks to examine the true effect of PMS concentration on the degradation of HA. The experimental conditions were established as follows: UV radiation intensity (I_0) was set at 3.28 mW/cm^2 , the initial concentration of HA was 10 mg/L , the solution temperature was maintained at $25 \pm 3 \text{ }^\circ\text{C}$, the stirring speed was set at 630 rpm , and the initial pH was adjusted to 5. The PMS oxidant was introduced at concentrations of 1 mmol/L , 2 mmol/L , 3 mmol/L , 4 mmol/L , 5 mmol/L , and 6 mmol/L . The experiment was carried out for a duration of 180 min to investigate the effect of varying PMS concentrations on the degradation of HA in UV/PMS system. The experimental results are depicted in Figure 14.

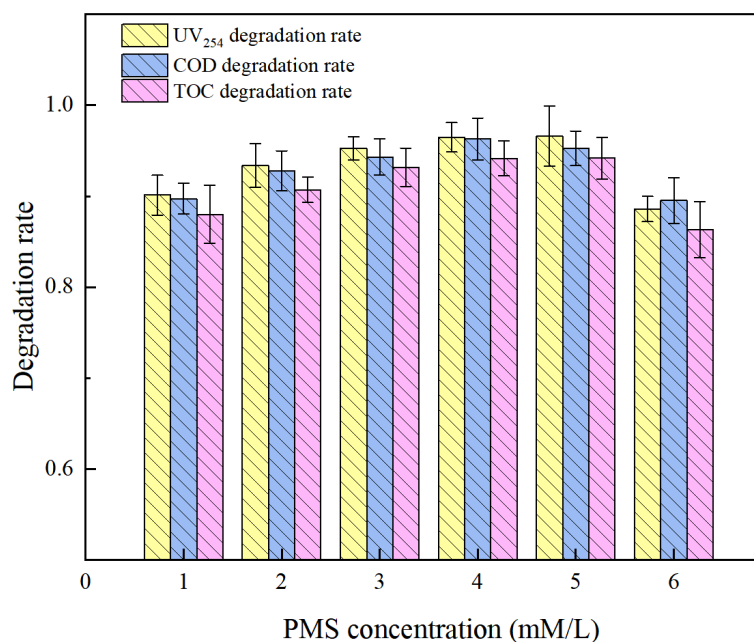
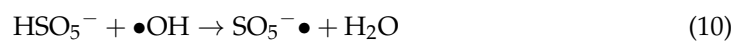
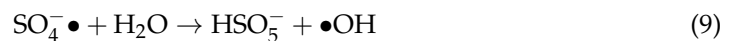


Figure 14. Effect of PMS concentration on degradation efficiency of organic matter.

In Figure 14, the degradation efficiencies of UV₂₅₄, COD, and TOC exhibited a continuous increase with the rise in oxidant concentration at low levels of PMS (1 mM/L , 2 mM/L , 3 mM/L , 4 mM/L), eventually reaching peak values of 96.47% , 96.29% , and

94.16%, respectively. The efficiency of UV₂₅₄ degradation exceeded that of TOC, suggesting that selective oxidants exhibit a higher reactivity towards UV₂₅₄ or fluorescent additives (e.g., aromatic groups). Higher concentrations of oxidants typically result in increased degradation efficiencies of organic matter [44]. However, upon surpassing a PMS concentration of 4 mM/L, a masking phenomenon was observed [45]. Consequently, the degradation efficiencies of UV₂₅₄, COD, and TOC decreased to 88.58%, 89.52%, and 86.31%, respectively. This decrease suggests an inhibitory effect of elevated oxidant concentrations on the degradation of HA. The analysis indicated that at elevated concentrations of PMS, there is an increased likelihood of quenching reactions occurring between radicals (Equations (9) and (10)) [46], as well as between excess persulfate and SO₄^{-•} and •OH (Equations (11) and (12)) [47]. This leads to a reduction in the reaction rate between radicals and HA, consequently affecting the degradation efficiency negatively.



Additionally, the efficiency of degradation is also affected by the technique of oxidant addition. The gradual and continuous addition of the oxidant to the reaction system can help to sustain the radical concentration within an optimal range, thereby enabling the continuous and efficient degradation of HA. This approach proves to be more effective compared to a single-dose addition.

3.6.4. Effect of HA Concentration

Under the specified experimental parameters, including I₀ of 3.28 mW/cm², a solution temperature of 25 ± 3 °C, a stirring speed of 630 rpm, an initial pH of 5, and a PMS concentration of 3 mmol/L, HA was synthesized at varying initial concentrations of 5 mg/L, 10 mg/L, 15 mg/L, 20 mg/L, and 25 mg/L. The experiment was carried out over a duration of 180 min to examine the effect of the concentration of HA on the efficacy of degradation in UV/PMS system. The experimental results are depicted in Figure 15.

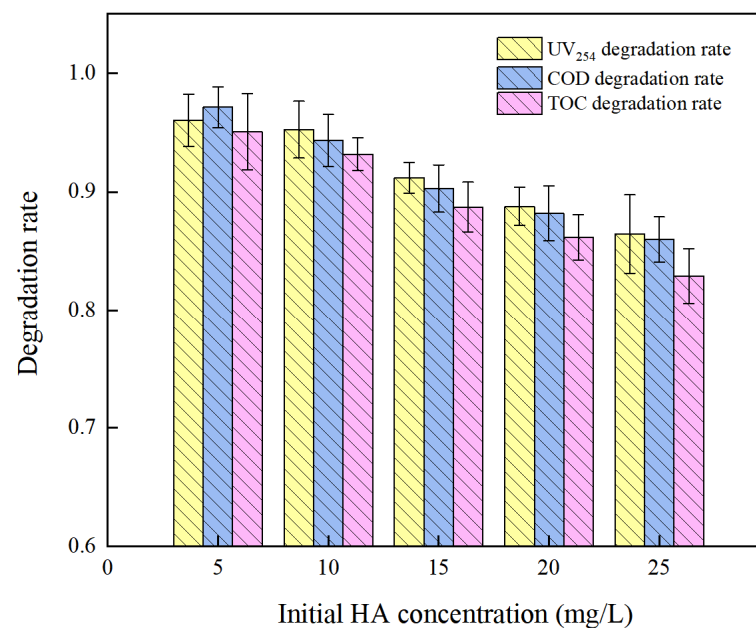


Figure 15. Effect of substrate concentration on degradation efficiency of organic matter.

In Figure 15, larger initial concentrations of HA led to decreased degradation efficiencies, without any discernible optimal concentration. When the initial concentration of HA was raised from 5 mg/L to 25 mg/L, the degradation efficiencies of UV₂₅₄, COD, and TOC decreased from 96.02%, 97.12%, and 95.05% to 86.44%, 85.98%, and 82.91%, respectively. In comparison to UV₂₅₄, the degradation efficiency of HA's TOC was found to be lower. This suggests that certain UV-absorbing units or fluorophores underwent partial oxidation to form low molecular weight compounds instead of complete mineralization [48]. Table 4 illustrates that elevated initial concentrations of HA lead to decreased degradation rates of organic matter.

Table 4. Kinetic fitting of HA degradation at different initial substrate concentrations.

HA	First-Order Kinetic Equation	k_{obs} (min^{-1})	R^2
5	$\text{Ln}(C_0/C) = 0.0167t + 0.7213$	0.0167	0.9841
10	$\text{Ln}(C_0/C) = 0.0149t + 0.6789$	0.0149	0.9812
15	$\text{Ln}(C_0/C) = 0.0121t + 0.6591$	0.0121	0.9936
20	$\text{Ln}(C_0/C) = 0.011t + 0.6139$	0.0110	0.9868
25	$\text{Ln}(C_0/C) = 0.0098t + 0.5631$	0.0098	0.9886

The sluggish elimination of HA can be attributed to several potential factors, including the following: ① A reduction in the quantity of oxidative radicals at a specific persulfate dosage and UV intensity level. As the concentration of organic matter increases, HA and its degradation byproducts compete for $\text{SO}_4^{\cdot-}$ and $\cdot\text{OH}$ radicals [49]. ② The augmentation of HA concentration results in a visual darkening of the solution, thereby diminishing its transparency. UV radiation is subsequently obstructed and assimilated by HA molecules and their decomposition intermediates, thereby impeding the activation of PMS [50]. ③ HA functions as a scavenger of $\text{SO}_4^{\cdot-}$ and $\cdot\text{OH}$, effectively consuming elevated quantities of reactive radicals [51]. Therefore, in scenarios with ample oxidants, increased concentrations of HA necessitate extended durations to attain equivalent degradation efficiencies.

In summary, within the specified parameters of UV radiation intensity $I_0 = 3.28 \text{ mW/cm}^2$, solution temperature of $25 \pm 3^\circ\text{C}$, stirring speed of 630 rpm, and initial HA concentration of 10 mg/L, a reaction duration of 180 min, the optimal conditions were identified as an initial reaction pH of 5 and PMS concentration of 3 mmol/L. Under the optimal conditions described, the highest removal efficiencies recorded were a COD degradation efficiency of 96.32%, UV₂₅₄ degradation efficiency of 97.34%, HA mineralization rate of 92.09%, and an *EE/O* of 0.0149 (kWh)/m³. Table 5 shows the comparison with previous studies.

Table 5. Degradation performance of HA by different UV/AOPs processes.

Processing	Concentration	pH	AOPs	Time	Degradation Rate	Reference
UV/PMS (H_2SO_5)	$2 \text{ mg}\cdot\text{L}^{-1}$	7	PDS: $0.5 \text{ mmol}\cdot\text{L}^{-1}$	180 min	100%	[10]
UV/SPC (Na_2CO_3)	$5 \text{ mg}\cdot\text{L}^{-1}$	9.9	SPC: $0.5 \text{ mmol}\cdot\text{L}^{-1}$	90 min	92.1%	[31]
UV/SPB (NaBO_3)	$10 \text{ mg}\cdot\text{L}^{-1}$	3	SPB: $1 \text{ mmol}\cdot\text{L}^{-1}$	60 min	88.8%	[39]
UV/ H_2O_2	$15 \text{ mg}\cdot\text{L}^{-1}$	4	H_2O_2 : $3 \text{ mmol}\cdot\text{L}^{-1}$	180 min	21.9%	[45]
UV/PDS ($\text{H}_2\text{S}_2\text{O}_8$)	$15 \text{ mg}\cdot\text{L}^{-1}$	6	PDS: $3 \text{ mmol}\cdot\text{L}^{-1}$	120 min	92.9%	[45]
UV/PMS (H_2SO_5)	$10 \text{ mg}\cdot\text{L}^{-1}$	3	PMS: $3 \text{ mmol}\cdot\text{L}^{-1}$	180 min	92.09%	This work

4. Conclusions

This study explored the degradation efficiency of HA through the utilization of UV₂₅₄, COD, TOC degradation efficiencies, and *EE/O* as economic metrics to evaluate and contrast the effectiveness of different UV/AOPs synergistic processes in comparison to individual processes. The results suggested that both the individual oxidant and UV processes exhibited significantly lower efficacy in treating HA in comparison to the synergistic

processes. Among the synergistic processes, UV/PMS exhibited the highest performance, achieving a mineralization rate of up to 94.15%, followed by UV/PDS and UV/SPC. The UV/S(IV) process exhibited the lowest effectiveness, achieving a mineralization rate of only 19.8%. Further exploration of the variables influencing the UV/PMS treatment of HA indicated that acidic environments were more favorable for the degradation of HA, with an optimum pH level of 3. The rate of HA degradation was determined to be directly proportional to the duration of illumination and inversely proportional to the initial concentration of the reactants. The optimal concentration of the oxidant was found to be 3 mmol/L. Under the experimental conditions with an initial concentration of 10 mg/L for HA, 3 mmol/L for PMS, and a starting pH of 5, the reaction was carried out for 180 min. The results showed significant degradation efficiencies: a COD degradation efficiency of 96.32%, a UV₂₅₄ degradation efficiency of 97.34%, HA mineralization rate of 92.09%, and an EE/O ratio of 0.0149 (kWh)/m³. The results illustrate the high efficacy of the UV/PMS synergistic system in the degradation and mineralization of HA in water.

Author Contributions: Conceptualization, Q.S. and X.S.; methodology, Q.S.; software, J.F.; validation, Q.S. and J.F.; formal analysis, Q.S.; investigation, C.C.; resources, Q.S.; data curation, Z.L.; writing—original draft preparation, Q.S.; writing—review and editing, X.S.; visualization, Q.S.; supervision, X.S.; project administration, X.S.; funding acquisition, X.S. All authors have read and agreed to the published version of the manuscript.

Funding: This study was supported by the Scientific Research Program for Higher Educational Institutions in Gansu Province (2020C-038), which is titled “Research on Key Technologies for Water Safety, Health Risk Prevention and Control and Domestic Waste Disposal in the Lanzhou Section of the Yellow River Basin”.

Data Availability Statement: All valid data are reflected in the article and authorized to be used.

Conflicts of Interest: The funders had no role in the design of the study; in the collection, analyses, or interpretation of data; in the writing of the manuscript, or in the decision to publish the results.

References

1. Reyes, T.G.; Crisosto, J.M. Characterization of dissolved organic matter in river water by conventional methods and direct sample analysis—time of flight-mass spectrometry. *J. Chem.* **2016**, *11*, 1537370. [[CrossRef](#)]
2. Vogt, R.D.; Garmo, Ø.A.; Austnes, K.; Kaste, Ø.; Haaland, S.; Sample, J.E.; Thrane, J.-E.; Skancke, L.B.; Gundersen, C.B.; de Wit, H.A. Factors Governing Site and Charge Density of Dissolved Natural Organic Matter. *Water* **2024**, *16*, 1716. [[CrossRef](#)]
3. Ryu, J.H.; Jung, J.H.; Park, K.Y.; Song, W.J.; Choi, B.G.; Kweon, J.H. Humic acid removal and microbial community function in membrane bioreactor. *J. Hazard. Mater.* **2021**, *417*, 126088. [[CrossRef](#)] [[PubMed](#)]
4. Tang, W.W.; Zeng, G.M.; Gong, J.L.; Liang, J.; Xu, P.; Zhang, C.; Huang, B.B. Impact of humic/fulvic acid on the removal of heavy metals from aqueous solutions using nanomaterials: A review. *Sci. Total Environ.* **2014**, *468*, 1014–1027. [[CrossRef](#)] [[PubMed](#)]
5. Raj, A.; Dash, S.; Karnena, M.K. A review on techniques used for removal of natural organic matter (NOM) from the water. *IJSREM* **2022**, *6*, 1–10. [[CrossRef](#)]
6. Cui, L.; Zhang, Y.Y.; He, K.Y.; Sun, M.M.; Zhang, Z.H. Ti₄O₇ reactive electrochemical membrane for humic acid removal: Insights of electrosorption and electrooxidation. *Sep. Purif. Technol.* **2022**, *293*, 121112. [[CrossRef](#)]
7. Bhatnagar, A.; Sillanpää, M. Removal of natural organic matter (NOM) and its constituents from water by adsorption—A review. *Chemosphere* **2017**, *166*, 497–510. [[CrossRef](#)] [[PubMed](#)]
8. Ruecker, A.; Uzun, H.; Karanfil, T.; Tsui, M.T.K.; Chow, A.T. Disinfection byproduct precursor dynamics and water treatability during an extreme flooding event in a coastal blackwater river in southeastern United States. *Chemosphere* **2017**, *188*, 90–98. [[CrossRef](#)]
9. Wang, L.; Wei, S.; Jiang, Z.E. Effects of humic acid on enhanced removal of lead ions by polystyrene-supported nano-Fe (0) nanocomposite. *Sci. Rep.* **2020**, *10*, 19663. [[CrossRef](#)]
10. Alayande, A.B.; Hong, S. Ultraviolet light-activated peroxymonosulfate (UV/PMS) system for humic acid mineralization: Effects of ionic matrix and feasible application in seawater reverse osmosis desalination. *Environ. Pollut.* **2022**, *307*, 119513. [[CrossRef](#)]
11. Chen, W.; Yu, H.Q. Advances in the characterization and monitoring of natural organic matter using spectroscopic approaches. *Water Res.* **2021**, *190*, 116759. [[CrossRef](#)] [[PubMed](#)]
12. Li, Q.M.; Li, X.; Zhou, C.Q.; Lu, C.C.; Liu, B.G.; Wang, G.X. Insight into oxidation and adsorption treatment of algae-laden water: Algal organic matter transformation and removal. *J. Chem. Eng.* **2021**, *420*, 129887. [[CrossRef](#)]

13. Mulyati, S.; Aprilia, S.; Muchtar, S.; Syamsuddin, Y.; Rosnelly, C.M.; Bilad, M.R.; Samsuri, S.; Ismail, N.M. Fabrication of Polyvinylidene Difluoride Membrane with Enhanced Pore and Filtration Properties by Using Tannic Acid as an Additive. *Polymers* **2022**, *14*, 186. [[CrossRef](#)] [[PubMed](#)]
14. Zhu, G.C.; Bian, Y.N.; Hursthouse, A.S.; Xu, S.N.; Xiong, N.N.; Wan, P. The role of magnetic MOFs nanoparticles in enhanced iron coagulation of aquatic dissolved organic matter. *Chemosphere* **2020**, *247*, 125921. [[CrossRef](#)]
15. Du, T.T.; Zhang, G.; Zou, J. Coupling photocatalytic and electrocatalytic oxidation towards simultaneous removal of humic acid and ammonia–nitrogen in landscape water. *Chemosphere* **2022**, *286*, 131717. [[CrossRef](#)] [[PubMed](#)]
16. Giannakoudakis, D.A.; Qayyum, A.; Barczak, M.; Colmenares-Quintero, R.F.; Borowski, P.; Triantafyllidis, K.; Colmenares, J.C. Mechanistic and kinetic studies of benzyl alcohol photocatalytic oxidation by nanostructured titanium (hydro)oxides: Do we know the entire story? *Appl. Catal. B Environ.* **2023**, *320*, 121939. [[CrossRef](#)]
17. Asria, M.; Naghizadehb, A.; Hasania, A.; Mortazavi-Derazkolab, S.; Javida, A.; Masoudic, F. Sustainable green synthesis of ZnFe₂O₄@ZnO nanocomposite using Oleaster tree bark methanolic extract for photocatalytic degradation of aqueous humic acid in the presence of UV irradiation. *Water Supply Res. Technol.* **2023**, *72*, 1800–1814. [[CrossRef](#)]
18. Xu, L.; Zhou, Z.; Graham, N.J.; Liu, M.J.; Yu, W.Z. Enhancing ultrafiltration performance by gravity-driven up-flow slow biofilter pre-treatment to remove natural organic matters and biopolymer foulants. *Water Res.* **2021**, *195*, 117010. [[CrossRef](#)] [[PubMed](#)]
19. Lado Ribeiro, A.R.; Rodríguez-Chueca, J.J.; Giannakis, S. Urban and industrial wastewater disinfection and decontamination by advanced oxidation processes(AOPs): Current issues and future trends. *Water* **2021**, *13*, 560. [[CrossRef](#)]
20. Barisci, S.; Suri, R. Removal of polyfluorinated telomer alcohol by advanced oxidation processes(AOPs) in different water matrices and evaluation of degradation mechanisms. *J. Water Process Eng.* **2020**, *39*, 101745. [[CrossRef](#)]
21. Cao, Y.J.; Ren, Y.J.; Zhang, Q.F.; Zhao, M.M.; Bai, C.X.; Wang, T.F. Research Progress of UV-Advanced Oxidation for Treatment of Natural Organic Matters, China. *Chem. Biol. Eng.* **2022**, *39*, 1–5.
22. GB 11892-891; Water Quality-Determination of Permanganate Index. National Standard of the People's Republic of China: Beijing, China, 1990.
23. Yang, J.L.; Zhu, M.S.; Dionysiou, D.D. What is the role of light in persulfate-based advanced oxidation for water treatment? *Water Res.* **2021**, *189*, 116627. [[CrossRef](#)] [[PubMed](#)]
24. Liu, G.Y. Study on the Transformation and Mechanism of Organic Matter in Secondary Effluent in Ultraviolet Persulfate System. Master's Thesis, Beijing University of Chemical Engineering, Beijing, China, 2022.
25. Wang, J.; Wang, S. Activation of persulfate (PS) and peroxymonosulfate (PMS) and application for the degradation of emerging contaminants. *Chem. Eng. J.* **2018**, *334*, 1502–1517. [[CrossRef](#)]
26. Liu, B.H.; Ye, M.T.; Ren, Z.X.; Lichtfouse, E.; Chen, Z.B. Towards synergistic combination of biochar/ultrasonic persulfate enhancing removal of natural humic acids from water. *J. Environ. Chem. Eng.* **2022**, *10*, 107809. [[CrossRef](#)]
27. Sun, H.Y.; Xing, R.Z.; Ye, X.Y.; Yin, K.K.; Zhang, Y.L.; Chen, Z.; Zhou, S.G. Reactive oxygen species accelerate humification process during iron mineral-amended sludge composting. *Bioresour. Technol.* **2023**, *370*, 128554. [[CrossRef](#)] [[PubMed](#)]
28. Wang, Q.; Wang, T.; Laila, N.; Huang, K.; Wang, X.W.; Lei, R.; Bai, X.Y.; Xu, Q.Y. Carbon dots/TiO₂ enhanced visible light-assisted photocatalytic of leachate: Simultaneous effects and Mechanism insights. *Water Res.* **2023**, *245*, 120659. [[CrossRef](#)] [[PubMed](#)]
29. Lee, J.; von Gunten, U.; Kim, J.H. Persulfate-based advanced oxidation: Critical assessment of opportunities and roadblocks. *Environ. Sci. Technol.* **2020**, *54*, 3064–3081. [[CrossRef](#)] [[PubMed](#)]
30. Sun, X.Y. Removal of Reclaimed Water Disinfection by-Product Precursors Based on Uv Advanced Oxidation Technology. Master's Thesis, Shandong Construction University, Jinan, China, 2020.
31. Yuan, D.; Tang, J.; Nie, Z.; Tang, S. Study on the removal of humic acid from water by ultraviolet activated sodium percarbonate, China. *Yanshan Univ.* **2021**, *45*, 220–226.
32. Bremner, D.H.; Molina, R.; Martínez, F.; Melero, J.A.; Segura, Y. Degradation of phenolic aqueous solutions by high frequency sono-Fenton systems (US-Fe₂O₃/SBA-15-H₂O₂). *Appl. Catal. B Environ.* **2009**, *90*, 380–388. [[CrossRef](#)]
33. Li, Y.; Dong, H.; Li, L.; Xiao, J.; Xiao, S.; Jin, Z. Efficient degradation of sulfamethazine via activation of percarbonate by chalcopyrite. *Water Res.* **2021**, *202*, 117451. [[CrossRef](#)]
34. Liu, W.K.; Liu, B.; Li, X. UV/Fe(II) synergistically activated S(IV) per-treatment on HA-enhanced Ca²⁺ scaling in NF filtration: Fouling mitigation, mechanisms and correlation analysis of membrane resistance in different filtration stage. *Chemosphere* **2022**, *308*, 136302. [[CrossRef](#)] [[PubMed](#)]
35. Cao, Y.; Qiu, W.; Li, J.; Zhao, Y.M.; Jiang, J.; Pang, S. Sulfite enhanced transformation of iopamidol by UV photolysis in the presence of oxygen: Role of oxysulfur radicals. *Water Res.* **2021**, *189*, 116625. [[CrossRef](#)] [[PubMed](#)]
36. Devi, L.G.; Srinivas, M.; Arunakumari, M.L. Heterogeneous advanced photo-Fenton process using peroxymonosulfate and peroxydisulfate in presence of zero valent metallic iron: A comparative study with hydrogen peroxide photo-Fenton process. *J. Water Process Eng.* **2016**, *13*, 117–126. [[CrossRef](#)]
37. Wu, P.; Liu, Z.Y.; Stroet, M.; Liao, J.L.; Chai, Z.F.; Mark, A.E.; Ning, L.; Wang, D.Q. Understanding the Effect of pH on the Solubility and Aggregation Extent of Humic Acid in Solution by Combining Simulation and the Experiment. *Environ. Sci. Technol.* **2022**, *56*, 917–927.
38. Wang, W.Y.; Li, R.H.; Bu, F.; Gao, Y.; Gao, B.Y.; Yue, Q.Y.; Yang, M.; Li, Y. Coagulation and membrane fouling mechanism of Al species in removing humic acid: Effect of pH and a dynamics process analysis. *Sep. Purif. Technol.* **2023**, *309*, 123130. [[CrossRef](#)]

39. Yuan, D.L.; Zhai, Z.H.; Zhu, E.Y.; Liu, H.L.; Jiao, T.F.; Tang, S.F. Humic Acid Removal in Water via UV Activated Sodium Perborate Process. *Coatings* **2022**, *12*, 885. [[CrossRef](#)]
40. Lominchar, M.A.; Santos, A.; Miguel, E.D.; Romero, A. Remediation of aged diesel contaminated soil by alkaline activated persulfate. *Sci. Total Environ.* **2018**, *622–623*, 41–48. [[CrossRef](#)] [[PubMed](#)]
41. Lu, Q.; Liu, Y.Z.; Li, B.H.; Feng, L.; Du, Z.W.; Zhang, L.Q. Reaction kinetics of dissolved black carbon with hydroxyl radical, sulfate radical and reactive chlorine radicals. *Sci. Total Environ.* **2022**, *828*, 153984. [[CrossRef](#)] [[PubMed](#)]
42. Meng, J.Z.; Yuan, S.J.; Wang, W.; Jin, J.L.; Zhan, X.M.; Xiao, L.W.; Hu, Z.H. Photodegradation of roxarsone in the aquatic environment: Influencing factors, mechanisms, and artificial neural network modeling. *Environ. Sci. Pollut. Res.* **2021**, *29*, 7844–7852. [[CrossRef](#)]
43. Ji, G.X. Characterization of the Removal of Natural Organic Matter from Source Water by Ultraviolet/Peroxysulfate Advanced Oxidation Technology. Master's Thesis, Shandong Construction University, Jinan, China, 2020.
44. Mengge, F.; Xin, Y.; Qingqing, K.; Lei, Y.; Zhang, X.R.; Aghdam, E.; Yin, R.; Shang, C. Sequential ClO₂-UV/chlorine process for micropollutant removal and disinfection byproduct control. *Sci. Total Environ.* **2022**, *806*, 150354.
45. Tang, S.; Tang, J.; Yuan, D.; Wang, Z.; Zhang, Y.; Rao, Y. Elimination of humic acid in water: Comparison of UV/PDS and UV/PMS. *RSC Adv.* **2020**, *10*, 17627–17634. [[CrossRef](#)] [[PubMed](#)]
46. Wang, Z.M.; Chen, J.B.; Zhang, L.M.; Li, W.W.; Huang, T.Y. Activated Carbon Supported Co₃O₄ Catalysts to Activate Peroxy-monosulfate for Orange, G Degradation. *Huan Jing Ke Xue* **2016**, *37*, 2591–2600.
47. Jiang, F.; Qiu, B.; Sun, D. Advanced degradation of refractory pollutants in incineration leachate by UV/Peroxymonosulfate. *Chem. Eng. J.* **2018**, *349*, 338–346. [[CrossRef](#)]
48. Juan, L.; Yang, S.; Jin, J.; Yang, T.; Cao, Y. Oxidative treatment of NOM by selective oxidants in drinking water treatment and its impact on DBP formation in postchlorination. *Sci. Total Environ.* **2022**, *858*, 159908.
49. Xia, G.; Huang, Y.; Li, F.; Wang, L.C.; Pang, J.B.; Li, L.W.; Wang, K. A thermally flexible and multi-site tactile sensor for remote 3D dynamic sensing imaging. *Front. Chem. Sci. Eng.* **2020**, *14*, 1039–1051. [[CrossRef](#)]
50. Li, X.; Wu, B.; Zhang, Q.; Xu, D.; Liu, Y.; Ma, F.; Gu, Q.; Li, F. Mechanisms on the impacts of humic acids on persulfate/Fe²⁺-based groundwater remediation. *Chem. Eng. J.* **2019**, *378*, 122142.
51. Ike, I.A.; Linden, K.G.; Orbell, J.D.; Duke, M. Critical review of the science and sustainability of persulphate advanced oxidation processes. *Chem. Eng. J.* **2018**, *338*, 651–669. [[CrossRef](#)]

Disclaimer/Publisher's Note: The statements, opinions and data contained in all publications are solely those of the individual author(s) and contributor(s) and not of MDPI and/or the editor(s). MDPI and/or the editor(s) disclaim responsibility for any injury to people or property resulting from any ideas, methods, instructions or products referred to in the content.